

The generalized Marshall-Olkin Lomax distribution with applications to AIDS and COVID-19 data

Alexsandro A. Ferreira

Universidade Federal de Pernambuco, Brazil.

alexsandro.ferreira.aaf@gmail.com

Gauss M. Cordeiro

Universidade Federal de Pernambuco, Brazil.

gauss@de.ufpe.br

Abstract

The generalized Marshall-Olkin Lomax distribution is introduced, and its properties are easily obtained from those of the Lomax distribution. A regression model for censored data is proposed. The parameters are estimated through maximum likelihood, and consistency is verified by simulations. Three real datasets are selected to illustrate the superiority of the new models compared to those from two well-known classes.

Keywords: Censored data, COVID-19, Quantile function, Regression model

1 Introduction

Extended continuous distributions are essential in data analysis since it is possible to deal with different shapes in various fields. The Lomax distribution is widely applied in many areas, such as income and wealth inequality, biological sciences, lifetime and reliability, engineering, and actuarial sciences (Murthy et al., 2004; Corbellini et al., 2010; Alnssyan, 2023).

Recently, there has been a growing interest in exploring extensions of the Lomax distribution. These extensions are designed to enhance its flexibility and to model an even broader range of data more effectively. Some new extensions include the Marshall-Olkin Lomax (MOL) (Ghitany et al., 2007), beta Lomax (BL) (Rajab et al., 2013), transmuted exponentiated Lomax (Ashour and Eltehiwy, 2013), Kumaraswamy Lomax (KL) (Shams, 2013), gamma Lomax (Cordeiro et al., 2015), exponential Lomax (El-Bassiouny et al., 2015), Weibull Lomax (WL) (Tahir et al., 2015), Topp-Leone Lomax (Oguntunde et al., 2019), and Maxwell Lomax (Abiodun and Ishaq, 2022) distributions, among others.

Generating new distributions from compounding ones makes sense when there is enough novelty in the generated model and new and interesting properties, and it gives superior fits to real data than other generators. This is the case of this article, which introduces the *generalized Marshall-Olkin Lomax* (GMOL) distribution, which follows from the generator proposed by Chesneau et al. (2022) and the Lomax distribution. The GMO generator, although recent and not yet well-known as the beta-G (B-G) (Eugene et al., 2002) and

Kumaraswamy-G (K-G) (Cordeiro and de Castro, 2011) classes, has significant potential. All these generators have two additional parameters. According to Selim (2020), the B-G and K-G generators have each produced more than 100 special distributions. Their popularity and extensive use show their robustness and flexibility in modeling diverse data sets. However, the emergence of the GMO generator represents an extremely attractive alternative in this field. This underscores the importance of exploring and understanding various generators in statistical analysis, as even those less known can offer substantial benefits in specific contexts.

The objectives of the article are to present the GMOL distribution, a more flexible model than the Lomax, BL, and KL, find a linear representation to determine its main properties, implement a regression model for censored data, apply the maximum likelihood method to estimate the parameters, and evaluate the performance of the new models through simulations and three applications to real data.

The article unfolds as follows: Section 2 presents the GMOL distribution. Section 3 provides a linear representation of its density function and properties. Section 4 employs a regression model. Section 5 reports some simulations. Applications to real data are discussed in Section 6, and conclusions in Section 7.

2 The GMOL model

Let $\alpha \in (0, 1]$, $\lambda \in [0, 1]$, and $G(x) = G(x; \boldsymbol{\xi})$ be the cumulative distribution function (CDF) of any distribution with parameter vector $\boldsymbol{\xi}$. The GMO CDF, an alternative to the B-G and K-G families, can be expressed as (for $x \in \mathbb{R}$)

$$F(x) = F(x; \alpha, \lambda, \boldsymbol{\xi}) = \frac{\lambda G(x) + (1 - \lambda) G(x)^2}{\alpha + (1 - \alpha) G(x)}. \quad (1)$$

The CDF and probability density function (PDF) of the Lomax distribution (with parameters $\tau > 0$ and $\beta > 0$), say $\text{Lomax}(\tau, \beta)$, are given by (for $x > 0$)

$$G(x; \tau, \beta) = 1 - [\beta(\beta + x)^{-1}]^\tau, \quad (2)$$

and

$$g(x; \tau, \beta) = \frac{\tau \beta^\tau}{(\beta + x)^{\tau+1}}. \quad (3)$$

Inserting (2) in Equation (1) leads to the GMOL CDF

$$F(x) = \frac{\lambda \{1 - [\beta(\beta + x)^{-1}]^\tau\} + (1 - \lambda) \{1 - [\beta(\beta + x)^{-1}]^\tau\}^2}{\alpha + (1 - \alpha) \{1 - [\beta(\beta + x)^{-1}]^\tau\}}.$$

The corresponding PDF and HRF can be written as

$$f(x) = \frac{\tau \beta^\tau (1 - \alpha)(1 - \lambda) \{1 - [\beta(\beta + x)^{-1}]^\tau\}^2 + 2\alpha(1 - \lambda) \{1 - [\beta(\beta + x)^{-1}]^\tau\} + \alpha\lambda}{(\beta + x)^{\tau+1} [\alpha + (1 - \alpha) \{1 - [\beta(\beta + x)^{-1}]^\tau\}]^2}, \quad (4)$$

and

$$h(x) = \frac{\tau \beta^\tau (1 - \alpha)(1 - \lambda) [1 - [\beta(\beta + x)^{-1}]^\tau]^2 + 2\alpha(1 - \lambda) [1 - [\beta(\beta + x)^{-1}]^\tau] + \alpha\lambda}{(\beta + x)^{\tau+1} [\alpha + (1 - \lambda) \{1 - [\beta(\beta + x)^{-1}]^\tau\}] [\alpha + (1 - \alpha) \{1 - [\beta(\beta + x)^{-1}]^\tau\}]}$$

Henceforth, let $X \sim \text{GMOL}(\alpha, \lambda, \tau, \beta)$ have the PDF (4). The GMOL distribution accommodates some special cases. For instance, it reduces to the MOL model when $\lambda = 1$. For $|\lambda| \leq 1$ and $\alpha = 1$, it becomes the transmuted Lomax (Ashour and Eltehiwy, 2013). For $\lambda = 1$ and $\alpha = 1/2$, it is identical to a special case of the M Lomax (Kumar et al., 2017). Finally, if $\lambda = \alpha = 1$, it corresponds to the Lomax. Figure 1 displays the density and hazard rate shapes of the GMOL model.

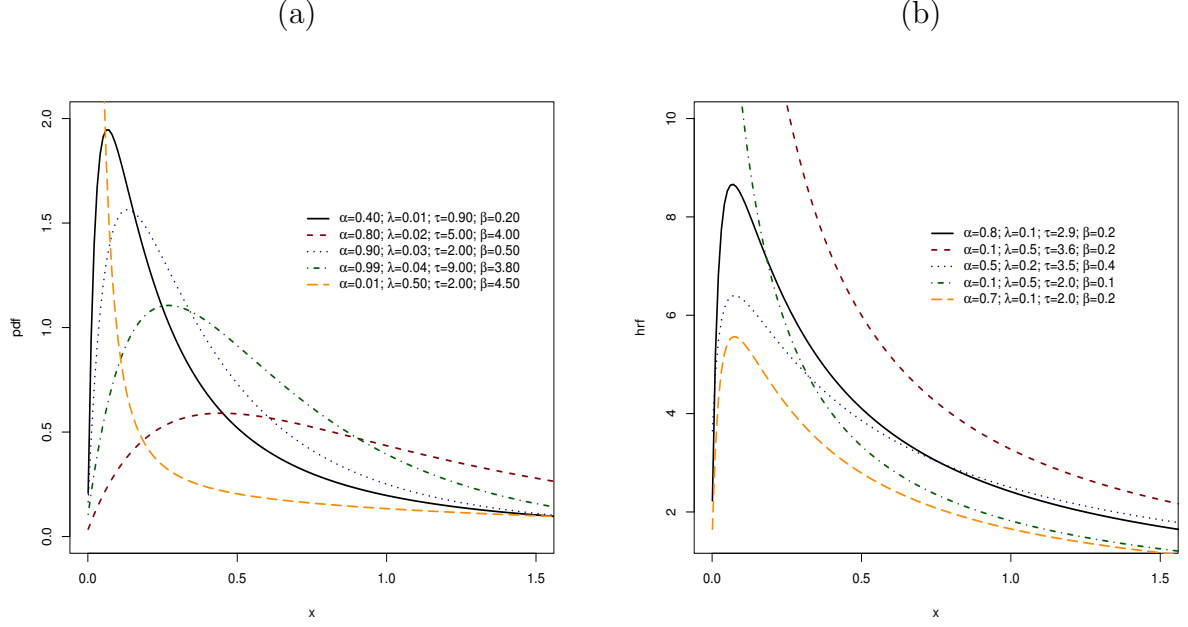


Figure 1: Density and HRF of X .

3 Properties

3.1 Linear representation

First, the generalized binomial expansion for $|v| < 1$, and $q \in \mathbb{R}$, is given by

$$(1 - v)^q = \sum_{j=0}^{\infty} (-1)^j \binom{q}{j} v^j, \quad (5)$$

where $\binom{q}{0} = 1$ and $\binom{q}{j} = \frac{1}{j!} \prod_{n=1}^j (q - n + 1)$ (for $j \geq 1$).

The PDF associated with (1) follows from Theorem 1 of Chesneau et al. (2022) as

$$f(x) = g_0(x) + \sum_{i=0}^{\infty} \sum_{j=0}^{i+1} \omega_{i,j} g_j(x), \quad (6)$$

where $g_j(x) = (j+1) g(x) G(x)^j$ is the exponentiated-G density with power $(j+1)$, and

$$\omega_{i,j} = (-1)^j (\lambda - \alpha)(1 - \alpha)^i \binom{i+1}{j}.$$

Further, we can write (6) as

$$f(x) = g_0(x) + \sum_{j=0}^{\infty} \rho_j g_j(x), \quad (7)$$

where $\rho_j = \sum_{i=\delta_j}^{\infty} \omega_{i,j}$, and $\delta_0 = \delta_1 = 0$ and $\delta_j = j - 1$ for $j \geq 2$. Thus, substituting (2) and (3) in Equation (7), the PDF of X reduces to

$$f(x) = \frac{\tau \beta^\tau}{(\beta + x)^{\tau+1}} + \sum_{j=0}^{\infty} \rho_j \frac{(j+1)\tau \beta^\tau}{(\beta + x)^{\tau+1}} \left\{ 1 - [\beta(\beta + x)^{-1}]^\tau \right\}^j. \quad (8)$$

Applying expansion (5) to the binomial term in (8),

$$f(x) = \frac{\tau \beta^\tau}{(\beta + x)^{\tau+1}} + \sum_{j=0}^{\infty} \rho_j \frac{(j+1)\tau \beta^\tau}{(\beta + x)^{\tau+1}} \sum_{k=0}^j (-1)^k \binom{j}{k} [\beta(\beta + x)^{-1}]^{k\tau}. \quad (9)$$

By rearranging the terms in (9) and changing $\sum_{j=0}^{\infty} \sum_{k=0}^j$ by $\sum_{k=0}^{\infty} \sum_{j=k}^{\infty}$,

$$f(x) = g(x; \tau, \beta) + \sum_{k=0}^{\infty} \varphi_k g(x; \tau^*, \beta), \quad (10)$$

where $\tau^* = (k+1)\tau$,

$$\varphi_k = \frac{(-1)^k}{(k+1)} \sum_{j=k}^{\infty} (j+1) \binom{j}{k} \rho_j,$$

and $g(x; \tau^*, \beta)$ is the PDF of the Lomax distribution with parameters τ^* and β . So, the GMOL properties follow from (10), and those Lomax properties.

3.2 Quantile function

The quantile function (qf) of X is (Chesneau et al., 2022) (for $0 < u < 1$)

$$Q_X(u) = \beta \left(\left\{ 1 - \left[\frac{(1-\alpha)u - \lambda + \sqrt{[\lambda - (1-\alpha)u]^2 + 4\alpha(1-\lambda)u}}{2(1-\lambda)} \right] \right\}^{-1/\tau} - 1 \right). \quad (11)$$

Plots of the Bowley skewness (Kenney and Keeping, 1962) and Moors kurtosis (Moors, 1988) of X obtained from (11) with τ and β fixed, and varying α and λ , are reported in Figure 2. The skewness and kurtosis of X change with the values of α and λ , where there is a peak (red region) indicating that these measures reach their maximum value.

3.3 Moments and generating function

The p th moment of the Lomax model is (Cordeiro et al., 2015)

$$\mu'_{p, \text{Lomax}} = \frac{\beta^p \Gamma(\tau - p) \Gamma(p+1)}{\Gamma(\tau)}, \quad p < \tau, \quad (12)$$

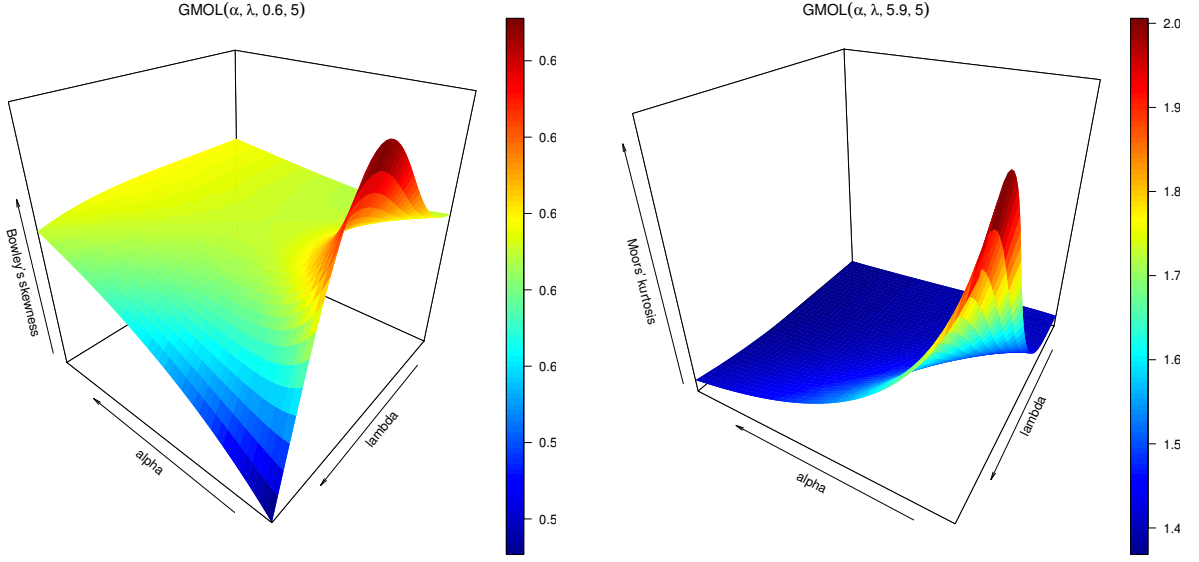


Figure 2: Skewness and kurtosis of X .

where $\Gamma(\cdot)$ is the complete gamma function. Thus, from Equations (10) and (12), the p th moment of X reduces to

$$\mu'_p = \frac{\beta^p \Gamma(\tau - p) \Gamma(p + 1)}{\Gamma(\tau)} + \sum_{k=0}^{\infty} \varphi_k \frac{\beta^p \Gamma(\tau^* - p) \Gamma(p + 1)}{\Gamma(\tau^*)}.$$

The p th incomplete moment of X , $m_p(s) = \int_0^s x^p f(x) dx$, follows from (10) as

$$m_p(s) = \int_0^s \frac{x^p \tau \beta^\tau}{(\beta + x)^{\tau+1}} dx + \sum_{k=0}^{\infty} \varphi_k \int_0^s \frac{x^p \tau^* \beta^{\tau^*}}{(\beta + x)^{\tau^*+1}} dx.$$

Next, by making a change of variable and using the upper incomplete beta function $B_z(a, b) = \int_z^1 t^{a-1} (1-t)^{b-1} dt$, the p th incomplete moment of X can be expressed as

$$m_p(s) = \tau \beta^p B_{\beta/(\beta+s)}(\tau - p, p + 1) + \sum_{k=0}^{\infty} \varphi_k \tau^* \beta^p B_{\beta/(\beta+s)}(\tau^* - p, p + 1).$$

The first incomplete moment of X provides the plots of the well-known Bonferroni and Lorenz curves. These curves versus the probability ν (varying α and λ) for $\tau = 6.0$ and $\beta = 2.0$, are given in Figure 3.

Further, two analytical expressions for the generating function (gf) of X are derived. First, from Equation (10),

$$M_X(t) = \mathbb{E}[\exp(tX)] = M_{\tau, \beta}(t) + \sum_{k=0}^{\infty} \varphi_k M_{\tau^*, \beta}(t), \quad (13)$$

where $M_{\tau, \beta}(t)$ and $M_{\tau^*, \beta}(t)$ are Lomax gfs with these parameters, namely

$$M_X(t) = \int_0^{\infty} \frac{e^{tx} \tau \beta^\tau}{(\beta + x)^{\tau+1}} dx + \sum_{k=0}^{\infty} \varphi_k \int_0^{\infty} \frac{e^{tx} \tau^* \beta^{\tau^*}}{(\beta + x)^{\tau^*+1}} dx.$$

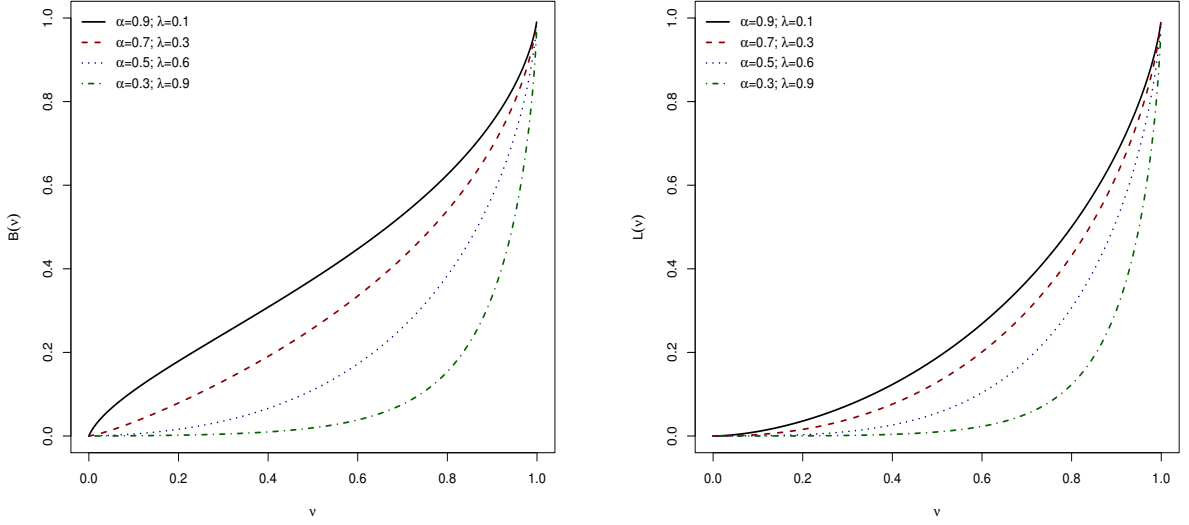


Figure 3: Bonferroni and Lorenz curves of X .

For the first integral above, following the findings of Lemonte and Cordeiro (2013), one has

$$M_{\tau,\beta}(t) = \int_0^\infty \frac{e^{tx}\tau\beta^\tau}{(\beta+x)^{\tau+1}} dx = \tau \int_0^\infty e^{t\beta y} (1+y)^{-(\tau+1)} dy.$$

Equations (9.210.1), (9.210.2), and (9.211.4) provided by Gradshteyn and Ryzhik (2007) are employed to express the Kummer function $\Psi(a, \gamma; z)$ as follows

$$\begin{aligned} \Psi(a, \gamma; z) &= \frac{1}{\Gamma(a)} \int_0^\infty e^{-zt} t^{a-1} (1+t)^{\gamma-(a+1)} dt \\ &= \frac{\Gamma(1-\gamma)}{\Gamma(1+a-\gamma)} {}_1F_1(a, \gamma; z) + \frac{\Gamma(1-\gamma)}{\Gamma(a)} {}_1F_1(1+a-\gamma, 2-\gamma; z), \end{aligned}$$

where

$${}_1F_1(a, \gamma; z) = \frac{\Gamma(\gamma)}{\Gamma(a)} \sum_{j=0}^{\infty} \frac{\Gamma(a+j)z^j}{\Gamma(\gamma+j)j!}$$

is the confluent hypergeometric function.

Then, for $t < 0$,

$$M_{\tau,\beta}(t) = \Psi(1, 1-\tau; -\beta t) = \tau^{-1} {}_1F_1(1, 1-\tau; -\beta t) + e^{-\beta t}. \quad (14)$$

Combining (14) and (13), the gf of X is

$$M_X(t) = \frac{1}{\tau} {}_1F_1(1, 1-\tau; -\beta t) + e^{-\beta t} + \sum_{k=0}^{\infty} \varphi_k \frac{1}{\tau^*} {}_1F_1(1, 1-\tau^*; -\beta t) + e^{-\beta t}.$$

The other representation follows from Lemonte and Cordeiro (2013) by taking $u = \beta/(\beta+x)$ in (3) and solving the resulting integral (for $t < 0$)

$$M_{\tau,\beta}(t) = -\tau \exp(-\beta t) (-\beta t)^\tau \left[\frac{\pi(\pi\tau)}{\Gamma(\tau+1)} + \Gamma(-\tau) - \Gamma(-\tau, -\beta t) \right], \quad t < 0, \quad (15)$$

where $\Gamma(\cdot, \cdot)$ is the upper incomplete gamma function. Combining Equations (13) and (15) leads to the gf of X .

3.4 Parameter estimation

Let x_1, \dots, x_n be independent and identically distributed (iid) observations from X . The log-likelihood function for $\boldsymbol{\theta} = (\alpha, \lambda, \tau, \beta)^\top$ is

$$\begin{aligned} \ell(\boldsymbol{\theta}) = & n \log(\tau \beta^\tau) + \sum_{i=1}^n \log \left\{ (1-\alpha)(1-\lambda) \left\{ 1 - [\beta(\beta+x_i)^{-1}]^\tau \right\}^2 \right. \\ & \left. + 2\alpha(1-\lambda) \left\{ 1 - [\beta(\beta+x_i)^{-1}]^\tau \right\} + \alpha\lambda \right\} - (\tau+1) \sum_{i=1}^n \log(\beta+x_i) \\ & - 2 \sum_{i=1}^n \log [\alpha + (1-\alpha) \left\{ 1 - [\beta(\beta+x_i)^{-1}]^\tau \right\}] . \end{aligned} \quad (16)$$

The maximum likelihood estimate (MLE) of $\boldsymbol{\theta}$ can be found by maximizing (16) using statistical programs. For instance, the AdequacyModel package (Marinho et al., 2019) in R simplifies this process by providing a range of optimization methods, including Broyden-Fletcher-Goldfarb-Shannon (BFGS), Nelder-Mead, and Simulated Annealing (SANN). To use this package, one only needs to supply the respective PDFs and CDFs of the models.

4 The GMOL regression model

In various real-world situations, the response variable can be affected by explanatory variables in both linear and nonlinear ways. The effects of these explanatory variables on the response variable can be evaluated through the parameters of position, scale, and shape. Recent research has introduced new regressions, such as those proposed by Prataviera et al. (2018), Prataviera et al. (2021), Biazatti et al. (2022), and Cordeiro et al. (2023). Following a similar approach, the GMOL regression model for censored samples is defined by the systematic components $\beta_i = \exp(\mathbf{v}_i^\top \boldsymbol{\eta}_1)$ and $\tau_i = \exp(\mathbf{v}_i^\top \boldsymbol{\eta}_2)$ for $i = 1, \dots, n$. Here, $\mathbf{v}_i^\top = (v_{i1}, \dots, v_{ir})^\top$ represents the vector of explanatory variables, while $\boldsymbol{\eta}_1 = (\eta_{11}, \dots, \eta_{1r})^\top$ and $\boldsymbol{\eta}_2 = (\eta_{21}, \dots, \eta_{2r})^\top$ denote the vectors of unknown parameters. Consequently, the survival function of $X_i | \mathbf{v}_i$ is

$$S(x | \mathbf{v}_i) = 1 - \frac{\lambda \left\{ 1 - [\beta_i(\beta_i+x)^{-1}]^{\tau_i} \right\} + (1-\lambda) \left\{ 1 - [\beta_i(\beta_i+x)^{-1}]^{\tau_i} \right\}^2}{\alpha + (1-\alpha) \left\{ 1 - [\beta_i(\beta_i+x)^{-1}]^{\tau_i} \right\}} .$$

Consider iid observations $(x_1, \mathbf{v}_1), \dots, (x_n, \mathbf{v}_n)$, where $x_i = \min(X_i, C_i)$, X_i is the lifetime, and C_i is the non-informative censoring time (assuming independence). For

right-censored data, the log-likelihood function for $\zeta = (\alpha, \lambda, \boldsymbol{\eta}_1^\top, \boldsymbol{\eta}_2^\top)^\top$ is

$$\begin{aligned}
\ell(\zeta) = & d \log(\tau_i \beta_i^{\tau_i}) + \sum_{i \in F} \log \left\{ (1 - \alpha)(1 - \lambda) \left\{ 1 - [\beta_i (\beta_i + x_i)^{-1}]^{\tau_i} \right\}^2 \right. \\
& + 2\alpha(1 - \lambda) \left\{ 1 - [\beta_i (\beta_i + x_i)^{-1}]^{\tau_i} \right\} + \alpha\lambda \left. \right\} - (\tau_i + 1) \sum_{i \in F} \log(\beta_i + x_i) \\
& - 2 \sum_{i \in F} \log [\alpha + (1 - \alpha) \left\{ 1 - [\beta_i (\beta_i + x_i)^{-1}]^{\tau_i} \right\}] \\
& + \sum_{i \in C} \log \left[1 - \frac{\lambda \left\{ 1 - [\beta_i (\beta_i + x_i)^{-1}]^{\tau_i} \right\} + (1 - \lambda) \left\{ 1 - [\beta_i (\beta_i + x_i)^{-1}]^{\tau_i} \right\}^2}{\alpha + (1 - \alpha) \left\{ 1 - [\beta_i (\beta_i + x_i)^{-1}]^{\tau_i} \right\}} \right], \tag{17}
\end{aligned}$$

where d is the number of failures, while F and C denote the lifetime and censoring sets, respectively. The MLE of ζ can be found by numerically maximizing (17).

5 Simulations

The MLEs of the parameters are calculated in three different scenarios with sample sizes ($n = 50, 100, 200$, and 300) generated from (11). The average estimates (AEs), biases, and mean squared errors (MSEs) are found from one thousand Monte Carlo replicates.

Table 1: Simulation findings from the new distribution.

n	θ	(0.2, 0.6, 0.5, 0.8)			(0.1, 0.3, 1.5, 3.0)			(0.5, 0.4, 9.0, 7.0)		
		AE	Bias	MSE	AE	Bias	MSE	AE	Bias	MSE
50	α	0.2137	0.0136	0.0147	0.1469	0.0469	0.0271	1.3720	0.8720	22.2787
	λ	0.5933	-0.0066	0.0416	0.3702	0.0702	0.0569	0.7306	0.3306	3.8829
	τ	0.5334	0.0334	0.0270	1.5495	0.0495	0.2730	10.1701	1.1701	48.8266
	β	0.8302	0.0302	0.0268	3.1355	0.1355	2.1256	7.4160	0.4160	6.7546
100	α	0.2098	0.0098	0.0057	0.1309	0.0309	0.0137	0.7853	0.2853	1.2737
	λ	0.6110	0.0110	0.0186	0.3570	0.0570	0.0474	0.5578	0.1578	0.3929
	τ	0.5131	0.0131	0.0112	1.5210	0.0210	0.0673	9.5443	0.5443	6.5548
	β	0.8230	0.0230	0.0094	3.1132	0.1132	0.2174	7.3049	0.3049	1.7086
200	α	0.2031	0.0031	0.0022	0.1219	0.0219	0.0045	0.6394	0.1394	0.3661
	λ	0.6099	0.0099	0.0067	0.3442	0.0442	0.0138	0.4931	0.0931	0.1298
	τ	0.5076	0.0076	0.0045	1.5170	0.0170	0.0245	9.3125	0.3125	1.2109
	β	0.8260	0.0260	0.0039	3.1030	0.1030	0.0685	7.2276	0.2276	0.5635
300	α	0.2030	0.0030	0.0010	0.1162	0.0162	0.0026	0.6001	0.1001	0.1726
	λ	0.6128	0.0128	0.0029	0.3372	0.0372	0.0082	0.4739	0.0739	0.0790
	τ	0.5047	0.0047	0.0023	1.5098	0.0098	0.0128	9.3029	0.3029	1.1190
	β	0.8255	0.0255	0.0021	3.1096	0.1096	0.0418	7.2178	0.2178	0.4575

The numbers in Table 1 reveal that the biases and MSEs decay and the AEs tend to

the true parameter values if n grows. This pattern confirms the consistency of the GMOL estimators.

One thousand Monte Carlo replicates are carried out for $n = 100, 200, 300$, and 500 to evaluate the MLEs in the regression model, whose parameters are: $\alpha = 0.5$, $\lambda = 0.3$, $\eta_{10} = 0.6$, $\eta_{11} = 0.8$, $\eta_{20} = 0.2$ and $\eta_{21} = 0.4$. The censoring times c_1, \dots, c_n are generated from a uniform $(0, b)$, leading to approximately 0% , 10% and 30% censoring.

The simulations follow the steps (for $i = 1, \dots, n$):

1. Generate $v_{i1} \sim \text{Uniform}(0, 1)$, and obtain $\beta_i = \exp(\eta_{10} + \eta_{11}v_{i1})$, and $\tau_i = \exp(\eta_{20} + \eta_{21}v_{i1})$.
2. Determine the lifetimes x_i^* from the $\text{GMOL}(\alpha, \lambda, \tau_i, \beta_i)$ model using Equation (11).
3. Generate $c_i \sim \text{Uniform}(0, b)$, and set $x_i = \min(x_i^*, c_i)$. If $x_i^* \leq c_i$ the censoring indicator $\delta_i = 1$. Otherwise, $\delta_i = 0$.

Table 2: Simulation findings from the new regression model.

n	ζ	0%			10%			30%		
		AE	Bias	MSE	AE	Bias	MSE	AE	Bias	MSE
100	α	0.9329	0.4328	7.7012	0.9751	0.4751	9.4838	1.0863	0.5863	21.1799
	λ	0.6504	0.3504	5.9446	0.6860	0.3860	7.3036	0.7851	0.4850	17.1892
	η_{10}	0.3656	-0.2344	2.3437	0.3609	-0.2391	3.1236	0.3536	-0.2463	4.1741
	η_{11}	0.6945	-0.1055	2.1605	0.6262	-0.1738	4.4126	0.5644	-0.2355	6.8824
	η_{20}	0.1738	-0.0262	1.3950	0.2038	0.0037	3.0267	0.1728	-0.0272	4.0611
	η_{21}	0.4886	0.0886	0.7776	0.5649	0.1649	1.8629	0.5409	0.1409	1.2378
200	α	0.6389	0.1389	3.2173	0.6766	0.1765	4.2393	0.8337	0.3337	5.0693
	λ	0.4185	0.1185	2.7730	0.4502	0.1501	3.6030	0.5968	0.2968	3.3692
	η_{10}	0.4976	-0.1024	2.6778	0.4783	-0.1216	1.6837	0.3388	-0.2612	1.0847
	η_{11}	0.7763	-0.0237	0.3780	0.7739	-0.0261	0.1149	0.7101	-0.0898	6.5198
	η_{20}	0.2286	0.0286	0.0650	0.2120	0.0120	1.4520	0.2079	0.0079	2.0934
	η_{21}	0.4674	0.0674	0.2637	0.4963	0.0963	0.0988	0.4988	0.0988	1.0179
300	α	0.5813	0.0813	0.5996	0.5808	0.0808	0.5558	0.6237	0.1237	1.7251
	λ	0.3658	0.0658	0.4516	0.3639	0.0639	0.4036	0.3639	0.1036	1.3717
	η_{10}	0.5443	-0.0557	0.4255	0.5503	-0.0496	0.5116	0.5504	-0.0883	1.5804
	η_{11}	0.7868	-0.0131	0.2021	0.7983	-0.0017	0.0371	0.7980	-0.0019	0.3882
	η_{20}	0.2269	0.0269	0.0293	0.2197	0.0197	0.0427	0.2143	0.0143	0.0769
	η_{21}	0.4486	0.0486	0.0522	0.4513	0.0513	0.0749	0.4574	0.0574	0.2823
500	α	0.5305	0.0305	0.0479	0.5309	0.0309	0.0548	0.5360	0.0360	0.0699
	λ	0.3209	0.0209	0.0283	0.3218	0.0218	0.0347	0.3249	0.0249	0.0430
	η_{10}	0.5850	-0.0149	0.0311	0.5851	-0.0148	0.0302	0.5855	-0.0144	0.0399
	η_{11}	0.8058	0.0058	0.0067	0.8082	0.0082	0.0076	0.8058	0.0058	0.0111
	η_{20}	0.2212	0.0212	0.0061	0.2167	0.0167	0.0100	0.2185	0.0185	0.0098
	η_{21}	0.4296	0.0296	0.0080	0.4311	0.0311	0.0102	0.4353	0.0353	0.0132

The numbers in Table 2 show that increasing the percentage of censoring, the biases and MSEs grow, negatively affecting their accuracy. However, larger samples mitigate

these effects, even in the presence of a high censoring percentage. In general, the AEs get closer to the real parameters, and the biases and MSEs converge to zero when n increases. This trend indicates the consistency of the GMOL regression estimators.

Equations (16) and (17) are optimized using the Nelder-Mead numerical method implemented in the `optim` function in R with numerical derivatives. The initial values of the parameters for both optimizations are set to their actual values. These simulation scripts are carried out without the use of any package in R.

6 Applications

The new models are applied to three real data sets. The Cramér-von Mises (W^*) and Anderson-Darling (A^*) statistics (Chen and Balakrishnan, 1995), Kolmogorov-Smirnov (KS) statistic with its p -value, as well as those well-known defined by the acronyms, are used to compare the fits of the models. The statistical analyses addressed in Sections 6.1 and 6.2 are carried out using the `AdequacyModel` package in R with the BFGS method. One of the main advantages of this package is its ability to calculate the MLEs, their standard errors (SEs), and various adequacy measures without the need to define the log-likelihood function. All that is required is to provide the PDF and CDF of the distribution that fits the data set. In Section 6.3, an R script is executed to obtain the results. This script requires the `GenSA` package to determine the initial values and employs the SANN numerical method via the `optim` function, whose output provides the MLEs, SEs, and adequacy measures for the chosen regressions fitted to the data.

6.1 AIDS data

The first data set refers to the time (in days) until the occurrence of opportunistic diseases in a cohort of 695 HIV-positive patients treated at the Hospital Universitário Gaffrée e Guinle (UNIRIO) in Rio de Janeiro, Brazil, between 1995 and 2002. These data were taken from the link <http://sobrevida.fiocruz.br/aidsoport.html>. The average time until the occurrence of opportunistic diseases is 520.062 days, accompanied by a substantial standard deviation of 608.729. The skewness (1.579) and kurtosis (5.135) indicate that the data are right-skewed and leptokurtic.

The GMOL distribution is compared with well-established distributions such as BL, KL, WL, MOL, and Lomax. The MLEs and their SEs (in parentheses) for the fitted models are shown in Table 3, which reveals that all distributions, except the BL and WL distributions, provide accurate estimates.

Table 4 reveals that the GMOL distribution has the lowest values of the adequacy measures, thus proving a good fit of the model to the data when compared to the alternative ones. In addition, the results of the generalized likelihood ratio (GLR) tests (Vuong, 1989) confirm the superiority of the GMOL model compared to the BL (GLR = 53.268), KL (GLR = 30.013), WL (GLR = 50.454), MOL (GLR = 35.174), and Lomax (GLR = 40.895) models at a 5% significance level. The plots in Figure 4 also support the numerical findings.

6.2 COVID-19 data (Paraíba)

The second data set consists of the lifetime (in days) of 109 individuals who died from COVID-19 in the state of Paraíba, Brazil, from 2020 to 2022, extracted from <https://op>

Table 3: Findings for AIDS data.

Model	MLEs (SEs)			
GMOL	0.137 (0.021)	0.493 (0.054)	48.753 (3.566)	34746.560 (1861.355)
BL	0.855 (0.038)	5.920 (15.363)	0.425 (1.114)	1044.264 (186.740)
KL	21.162 (1.705)	49.343 (9.962)	0.158 (0.010)	0.005 (0.001)
WL	0.019 (0.007)	1.628 (0.381)	0.428 (0.121)	1.179 (0.824)
MOL	0.754 (0.127)	2.512 (0.336)	1029.416 (256.111)	
Lomax	1.695 (0.136)	478.588 (55.623)		

Table 4: Adequacy measures for AIDS data.

Model	W^*	A^*	AIC	CAIC	BIC	HQIC	KS	p -value
GMOL	0.255	1.936	17173.830	17173.860	17194.170	17181.500	0.029	0.267
BL	0.780	5.676	17258.240	17258.270	17278.580	17265.900	0.048	0.006
KL	0.952	7.004	17281.970	17282.000	17302.310	17289.630	0.049	0.007
WL	0.427	3.165	17199.330	17199.370	17219.670	17207.000	0.039	0.051
MOL	0.808	5.933	17268.540	17268.560	17283.800	17274.290	0.054	0.001
Lomax	1.005	7.291	17291.050	17291.060	17301.220	17294.890	0.057	< 0.001

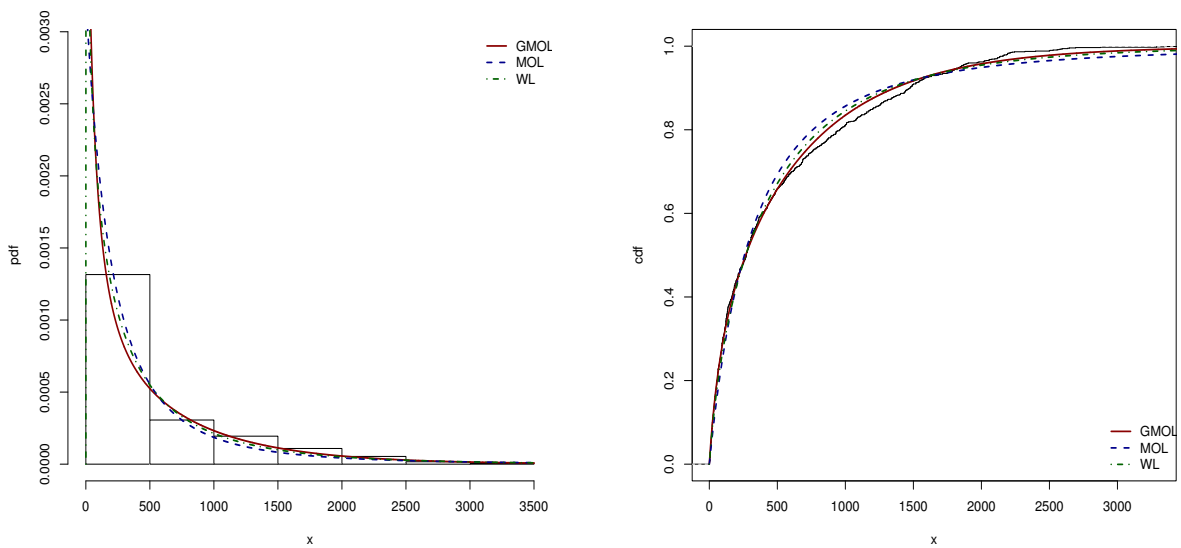


Figure 4: Estimated plots for AIDS data.

endatasus.saude.gov.br/dataset/notificacoes-de-sindrome-gripal-leve-2022. For these data, the average lifetime is 75.752 days, and the standard deviation is 100.251. The data are right-skewed and leptokurtic with skewness (1.641) and kurtosis (4.769).

The MLEs along with their SEs for the same fitted distributions discussed in Section 6.1 to the current data are provided in Table 5. The findings in Table 6 reveal the best fit of the GMOL model to these data. The GLR tests also indicate that the fit of the GMOL model is superior to its competitors, BL (GLR = 3.609), KL (GLR = 5.395), WL (GLR = 7.995), MOL (GLR = 12.997), and Lomax (GLR = 14.908), at a 5% significance level. These findings are visually confirmed by the plots in Figure 5. So, both numerically and visually, the GMOL model proves to be the most flexible fitted distribution to these COVID-19 data.

Table 5: Findings for COVID-19 data (Paraíba).

Model	MLEs (SEs)			
GMOL	0.088 (0.028)	0.604 (0.101)	65.508 (28.619)	8674.973 (3528.939)
BL	16.852 (13.933)	12.604 (17.752)	0.136 (0.142)	0.045 (0.108)
KL	6.015 (5.400)	23.973 (40.052)	0.149 (0.117)	0.116 (0.288)
WL	1.701 (8.636)	2.199 (1.466)	0.132 (0.245)	0.628 (1.004)
MOL	6.698 (0.223)	1.016 (0.846)	4.164 (130.195)	
Lomax	1.235 (0.324)	37.244 (16.420)		

Table 6: Adequacy measures for COVID-19 data (Paraíba).

Model	W^*	A^*	AIC	CAIC	BIC	HQIC	KS	p -value
GMOL	0.259	1.571	1128.321	1128.706	1139.087	1132.687	0.098	0.238
BL	0.320	1.893	1135.400	1135.785	1146.165	1139.766	0.130	0.047
KL	0.328	1.902	1134.235	1134.620	1145.001	1138.601	0.115	0.108
WL	0.326	1.880	1132.658	1133.043	1143.424	1137.024	0.102	0.204
MOL	0.415	2.411	1141.064	1141.293	1149.138	1144.338	0.116	0.103
Lomax	0.430	2.503	1141.193	1141.306	1146.576	1143.376	0.112	0.127

6.3 COVID-19 data (Distrito Federal)

The GMOL regression model is applied to a data set composed of 485 lifetimes (in days) of COVID-19 patients in Distrito Federal, Brazil, in 2020. This data can be accessed at the link: <https://covid19.ssp.df.gov.br/extensions/covid19/covid19.html>, which

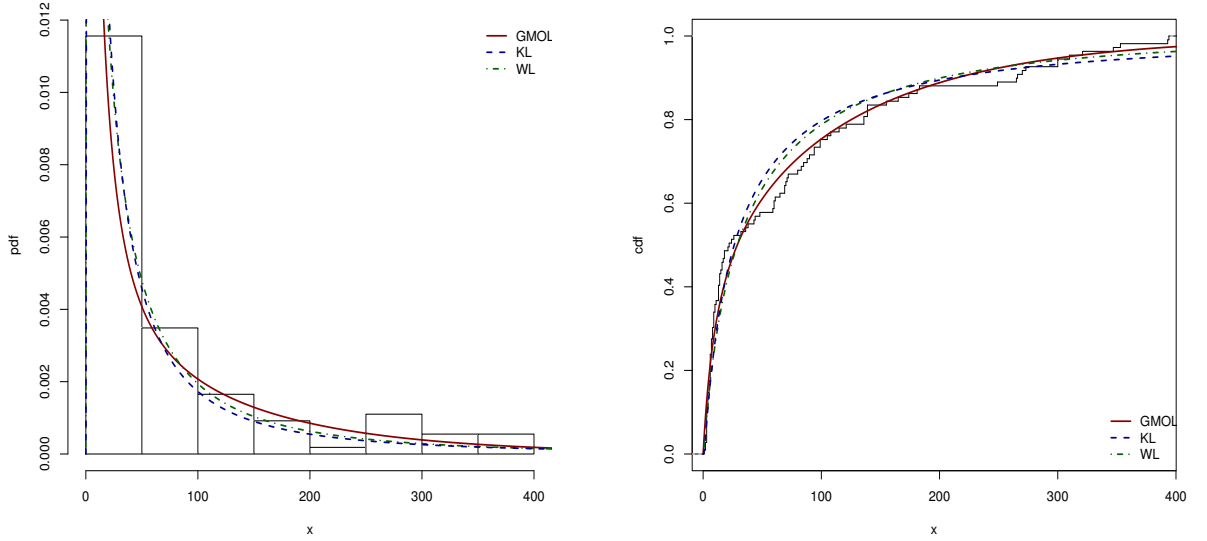


Figure 5: Estimated plots for COVID-19 data (Paraíba).

shows an average lifetime of 8.226 days with a standard deviation of 6.219. The skewness (1.155) and kurtosis (3.992) values show that the data are right-skewed and leptokurtic.

The response variable x_i corresponds to the time elapsed from the onset of symptoms until death from COVID-19 (failure). Approximately 78% of the observations are censored. The variables considered are (for $i = 1, \dots, 485$): δ_i : censoring indicator (0 = censored, 1 = lifetime observed), v_{i1} : age (in years), and v_{i2} : obesity (1 = yes, 0 = no or not informed).

In the GMOL model and its associated sub-models, namely MOL and Lomax, the explanatory variables are linked to systematic components as (for $i = 1, \dots, 485$)

$$\beta_i = \exp(\eta_{10} + \eta_{11}v_{i1} + \eta_{12}v_{i2}) \text{ and } \tau_i = \exp(\eta_{20} + \eta_{21}v_{i1} + \eta_{22}v_{i2}).$$

According to the numbers in Table 7, the GMOL model is the most suitable of the three fitted regression models to adjust COVID-19 data in Distrito Federal. In addition, the likelihood ratio (LR) tests support the superiority of the GMOL model over the others, as indicated by the rejection of the null hypotheses (Table 8).

The explanatory variables v_{i1} (η_{11}) and v_{i2} (η_{12}) are significant at the 5% level (Table 9), thus indicating that age and obesity are factors that can reduce the time to failure. In addition, both are significant for the variability of survival times (η_{21}) and (η_{22}). The residual analysis for the fitted GMOL regression model is done by the quantile residuals (qrs) (Dunn and Smyth, 1996)

$$qr_i = \Phi^{-1} \left(\frac{\hat{\lambda} \left\{ 1 - \left[\hat{\beta}_i (\hat{\beta}_i + x)^{-1} \right]^{\hat{\tau}_i} \right\} + (1 - \hat{\lambda}) \left\{ 1 - \left[\hat{\beta}_i (\hat{\beta}_i + x)^{-1} \right]^{\hat{\tau}_i} \right\}^2}{\hat{\alpha} + (1 - \hat{\alpha}) \left\{ 1 - \left[\hat{\beta}_i (\hat{\beta}_i + x)^{-1} \right]^{\hat{\tau}_i} \right\}} \right),$$

where $\Phi(\cdot)^{-1}$ is the qf of the standard normal distribution, $\hat{\beta}_i = \exp(\mathbf{v}_i^\top \hat{\boldsymbol{\eta}}_1)$ and $\hat{\tau}_i = \exp(\mathbf{v}_i^\top \hat{\boldsymbol{\eta}}_2)$. Figure 6 indicates a well-fitted regression model since the qrs have random behavior and approximately follow a standard normal distribution.

Table 7: Adequacy measures for COVID-19 data (Distrito Federal).

Model	AIC	CAIC	BIC	HQIC
GMOL	937.022	937.486	970.495	950.174
MOL	942.541	942.920	971.830	954.048
Lomax	943.274	943.576	968.379	953.137

Table 8: LR tests for COVID-19 data (Distrito Federal).

Model	Hypotheses	LR statistic	p-value
GMOL vs MOL	$H_0 : \lambda = 1$ vs $H_1 : H_0$ is false	7.5186	0.0061
GMOL vs Lomax	$H_0 : \alpha = \lambda = 1$ vs $H_1 : H_0$ is false	10.2516	0.0059

Table 9: Estimated results for COVID-19 data (Distrito Federal).

Parameter	MLEs	SEs	p-value
α	0.967	0.274	—
λ	0.143	0.069	—
η_{10}	10.248	2.010	<0.001
η_{11}	-0.097	0.025	0.001
η_{12}	-8.661	3.129	0.005
η_{20}	4.287	1.852	0.021
η_{21}	-0.048	0.021	0.027
η_{22}	-4.441	0.866	<0.001

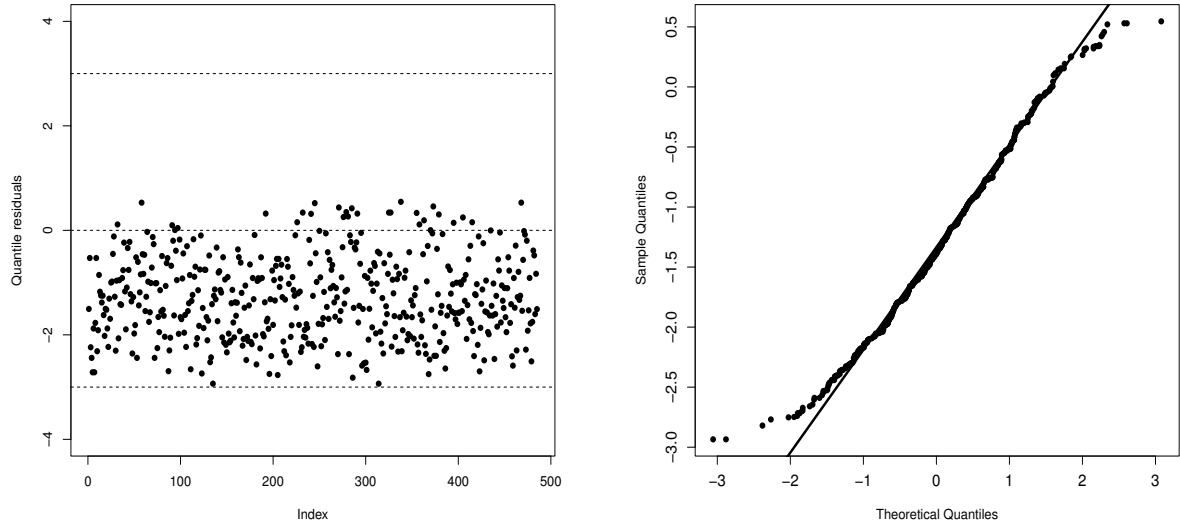


Figure 6: Index plot and normal probability plot for COVID-19 data (Distrito Federal).

7 Conclusions

This article presented the generalized Marshall-Olkin Lomax (GMOL) distribution, a more flexible alternative to the Lomax model. Its properties can be easily found from a linear representation in terms of Lomax densities. A regression model with two systematic components is proposed for censored data. Simulations confirm the consistency of the maximum likelihood estimators and the effectiveness of the regression model for censored data. The GMOL distribution outperformed the beta Lomax and Kumaraswamy Lomax models in real data analysis. Thus, this research contributed to the ongoing development of lifetime models and offered valuable tools for many diverse types of data.

Acknowledgments

Fundação de Amparo à Ciência e Tecnologia do Estado de Pernambuco (FACEPE) [IBPG-1448-1.02/20] supports this work.

References

Abiodun, A. A. and Ishaq, A. I. (2022). On Maxwell–Lomax distribution: properties and applications. *Arab Journal of Basic and Applied Sciences*, 29:221–232.

Alnssyan, B. (2023). The Modified-Lomax Distribution: Properties, Estimation Methods, and Application. *Symmetry*, 15:1367.

Ashour, S. and Eltehiwy, M. (2013). Transmuted exponentiated Lomax distribution. *Australian Journal of Basic and Applied Sciences*, 7:658–667.

Biazatti, E. C., Cordeiro, G. M., Rodrigues, G. M., Ortega, E. M. M., and de Santana, L. H. (2022). A Weibull-beta prime distribution to model COVID-19 data with the presence of covariates and censored data. *Stats*, 5(4):1159–1173.

Chen, G. and Balakrishnan, N. (1995). A general purpose approximate goodness-of-fit test. *Journal of Quality Technology*, 27:154–161.

Chesneau, C., Karakaya, K., Bakouch, H. S., and Kuş, C. (2022). An alternative to the Marshall-Olkin family of distributions: bootstrap, regression and applications. *Communications on Applied Mathematics and Computation*, 4:1229–1257.

Corbellini, A., Crosato, L., Ganugi, P., and Mazzoli, M. (2010). Fitting Pareto II distributions on firm size: Statistical methodology and economic puzzles. *Advances in Data Analysis: Theory and Applications to Reliability and Inference, Data Mining, Bioinformatics, Lifetime Data, and Neural Networks*, pages 321–328.

Cordeiro, G. M. and de Castro, M. (2011). A new family of generalized distributions. *Journal of Statistical Computation and Simulation*, 81:883–898.

Cordeiro, G. M., Ortega, E. M. M., and Popović, B. V. (2015). The gamma-Lomax distribution. *Journal of Statistical Computation and Simulation*, 85:305–319.

Cordeiro, G. M., Rodrigues, G. M., Ortega, E. M. M., de Santana, L. H., and Vila, R. (2023). An extended Rayleigh model: Properties, regression and covid-19 application. *Chilean Journal of Statistics*, 14(1):1–25.

Dunn, P. K. and Smyth, G. K. (1996). Randomized quantile residuals. *Journal of Computational and Graphical Statistics*, 5:236–244.

El-Bassiouny, A., Abdo, N., and Shahen, H. (2015). Exponential Lomax distribution. *International Journal of Computer Applications*, 121:24–29.

Eugene, N., Lee, C., and Famoye, F. (2002). Beta-normal distribution and its applications. *Communications in Statistics - Theory and Methods*, 31:497–512.

Ghitany, M. E., Al-Awadhi, F. A., and Alkhalfan, L. (2007). Marshall–Olkin extended Lomax distribution and its application to censored data. *Communications in Statistics—Theory and Methods*, 36:1855–1866.

Gradshteyn, I. S. and Ryzhik, I. M. (2007). *Table of integrals, series, and products*. Elsevier/Academic Press, Amsterdam, seventh edition. Translated from the Russian, Translation edited and with a preface by Alan Jeffrey and Daniel Zwillinger, With one CD-ROM (Windows, Macintosh and UNIX).

Kenney, J. and Keeping, E. (1962). *Moving averages*. 3 edn. NJ: Van Nostrand.

Kumar, D., Singh, U., Singh, S. K., and Mukherjee, S. (2017). The new probability distribution: an aspect to a life time distribution. *Math. Sci. Lett*, 6:35–42.

Lemonte, A. J. and Cordeiro, G. M. (2013). An extended Lomax distribution. *Statistics*, 47:800–816.

Marinho, P. R. D., Silva, R. B., Bourguignon, M., Cordeiro, G. M., and Nadarajah, S. (2019). AdequacyModel: An R package for probability distributions and general purpose optimization. *PLOS ONE*, 14:1–30.

Moors, J. J. A. (1988). A quantile alternative for kurtosis. *Journal of the Royal Statistical Society. Series D (The Statistician)*, 37:25–32.

Murthy, D. P., Xie, M., and Jiang, R. (2004). *Weibull models*, volume 505. John Wiley and Sons.

Oguntunde, P. E., Khaleel, M. A., Okagbue, H. I., and Odetunmibi, O. A. (2019). The Topp–Leone Lomax (TLLo) distribution with applications to airbone communication transceiver dataset. *Wireless Personal Communications*, 109:349–360.

Prataviera, F., Ortega, E. M. M., Cordeiro, G. M., Pescim, R. R., and Verssani, B. A. W. (2018). A new generalized odd log-logistic flexible Weibull regression model with applications in repairable systems. *Reliability Engineering & System Safety*, 176:13–26.

Prataviera, F., Silva, A. M. M., Cardoso, E. J. B. N., Cordeiro, G. M., and Ortega, E. M. M. (2021). A novel generalized odd log-logistic Maxwell-based regression with application to microbiology. *Applied Mathematical Modelling*, 93:148–164.

Rajab, M., Aleem, M., Nawaz, T., and Daniyal, M. (2013). On five parameter beta Lomax distribution. *Journal of Statistics*, 20:102–118.

Selim, M. A. (2020). The Distributions of Beta-Generated and Kumaraswamy-Generalized Families: A Brief Survey. *Figshare*, pages 1–19.

Shams, T. M. (2013). The Kumaraswamy-generalized lomax distribution. *Middle-East Journal of Scientific Research*, 17:641–646.

Tahir, M. H., Cordeiro, G. M., Mansoor, M., and Zubair, M. (2015). The Weibull-Lomax distribution: properties and applications. *Hacettepe Journal of Mathematics and Statistics*, 44:455–474.

Vuong, Q. H. (1989). Likelihood ratio tests for model selection and non-nested hypotheses. *Econometrica*, 57:307–333.